TRACKING TRANSVERSE 2D ULTRASOUND IMAGES OF THE CAROTID ARTERY

Conall Ó Gríofa, Jane Courtney
School of Electrical & Electronic Engineering
Dublin Institute of Technology
Dublin 8, Ireland
conall.ogriofa@gmail.com,
jane.courtney@dit.ie

Ciarán Finucane
TILDA
Trinity College Dublin
Dublin 2, Ireland
cfinuca@tcd.ie

Cleona Gray
Department of Vascular Surgery
Mater Misericordiae University Hospital Dublin
Dublin 7, Ireland
cgray@mater.ie

***Abstract*— This paper focuses on tracking transverse 2D ultrasound images as a means to produce a 3D representation of a bifurcating blood vessel in order to provide a foundation for autonomous aneurysm detection and classification, and atherosclerosis/atherosclerotic narrowing detection. In any healthcare system, a means to achieve the goal of automating point of care testing is desirable, especially given that a NHS study shows that 1.5% of men aged 65 studied had aortic diameters of greater than three centimeters [1]. In this paper, a method for creating a 3D representation of the carotid artery, determining and modeling the bifurcation region, and determining a subjects heart rate based on vascular distension in order to provide a foundation for autonomous point of care testing is presented.**

Keywords—Ultrasound; 3D Reconstruction; Motion Tracking; Active Contours

I. INTRODUCTION

According to the 2011-12 NHS (National Health Service) AAA Screening Programme Summary, 1.5% (of the sample size - 107051) of men aged 65 in the UK had aortic diameters of greater than the clinical threshold of three centimeters [1][2] which warrants a surveillance interval of twelve months under the NHS [3]. Screening currently requires manually guided ultrasound measurement of vessel diameter [4]. This is time consuming and can be subjective in nature leading to reliability issues. Given the critical clinical nature of this measurement and it's timeliness it is paramount that the methods employed are accurate, repeatable and time efficient.

The principle objectives outlined in this paper are to construct a three dimensional representation of an entire blood vessel (in this case the carotid artery) as a means of creating a foundation for autonomous aneurysm detection and autonomous atherosclerosis detection.

This is achieved by tracking the carotid artery(s) walls in a video sequence of two dimensional transverse ultrasound images using image processing techniques. This is performed in order to automatically detect the region in which the common carotid artery bifurcates into the external and internal carotid arteries.

Although the deliverables outlined in this paper could be translated to virtually any artery that bifurcates, the carotid artery was focus of this project.

The left and right common carotid arteries are the two main blood vessels that supply oxygenated blood to the brain. In general the carotid artery has three main components, the common carotid artery, the internal carotid artery and the external carotid artery.

The common carotid artery is the largest of the three components and it bifurcates into the smaller internal and external carotid arteries. The figure below shows what the average carotid artery should look like:

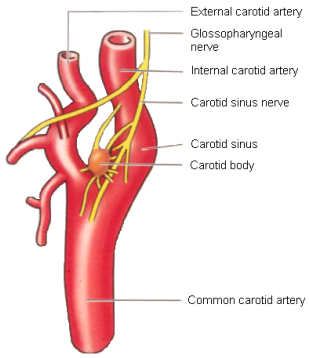

Figure 1: Anatomy of right carotid artery [5]

In [6], Finucane et al describe the anatomy of the carotid artery and provide a high level description of the image processing steps used. This is the most important paper with respect to this project, as it is the springboard to the project detailed in this paper.

Xin Yang's et al study [7] is centered around the analysis and segmentation of transverse ultrasound images of the carotid artery. This study involved segmenting the media adventitia and lumen intima boundaries of the carotid artery using Tim Cootes' et al statistical "Active Shape Model" segmentation technique [7][8]. In contrast with the project

around which this paper is written, Yang's et al study was performed using 3D ultrasound images/apparatus.

D. C . Barratt's et al study [9], similar to the study performed by Yang et al [7], involves segmenting the media adventitia and lumen intima boundaries. It differs from [7], however, as its geometric model is found using smoothing spines rather than the statistical active shape model.

The algorithms described in this paper are intended be a basis for further research in point of care applications including aneurysm detection and atherosclerosis detection among others.

II. METHODS

A. General Flow of Algorithm

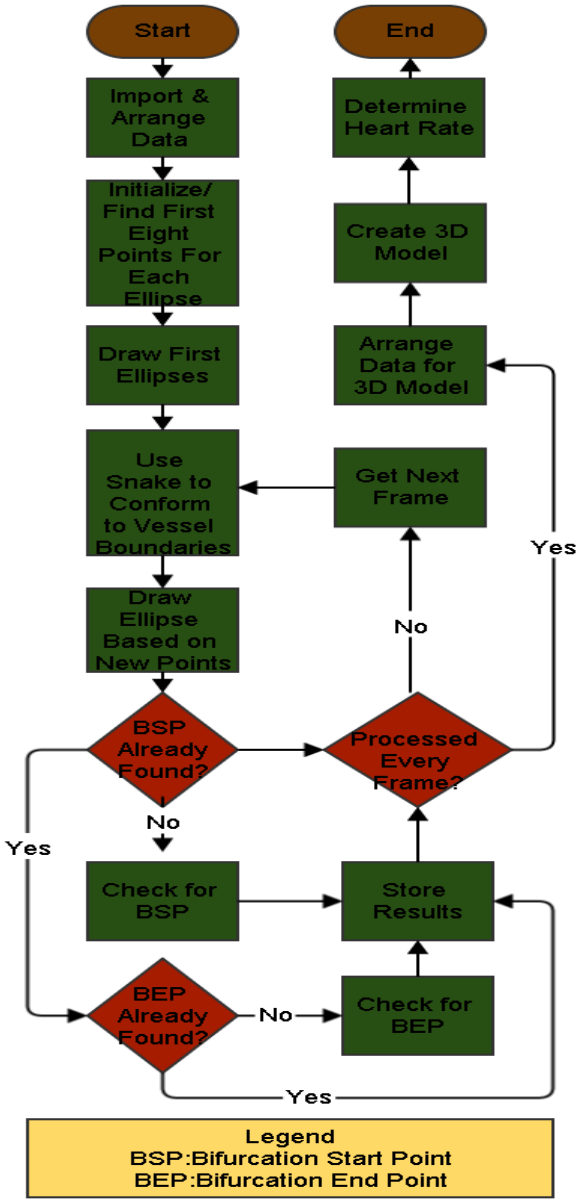

Figure 2: High level flow chart of algorithm

B. Arrangment & Importation of Data

The data used for the purposes of this paper was 2D transverse Doppler ultrasound data of the carotid artery in an uncompressed audio video interleaved (.avi) format.(for the version of Matlab being used - the appropriate codec was not available).

The ultrasounds of the carotid artery taken for the purposes of this paper, begin below the bifurcation at the common carotid artery and travel upwards past the bifurcation to show the internal and external carotid arteries.

This could potentially cause a technical issue as initially one object is to be tracked and then after the bifurcation, two objects are to be tracked. This may result in the common carotid artery being tracked correctly but after bifurcation the program could choose only one of the internal or external carotid arteries and track it twice rather than tracking both arteries.

The most simple solution to this issue was to flip the data and begin by tracking the external and internal carotid arteries and then the two tracking snakes can converge to the common carotid artery after the bifurcation.

C. Initialization

The initialization begins by sending the first frame of the data into initialization function.

The seed points that represent the centre of the internal and external carotid arteries are then found by firstly thresholding the image to specific constraints (certain HSV values).

This thresholding will lead to clusters of white that represent forward blood flow. The two largest white clusters are then determined and the (approximate) centre of each cluster is found.

The first image is then edge detected according to specific HSV values. The program then begins searching, starting from the seed points, for the first white pixel (which would denote an edge) in eight directions for each cluster centre.

The first eight edge points of each vessel are used to find the initial ellipses for each cluster using the least squares ellipse fitting algorithm developed by Courtney et al. [10].

D. Boundary Tracking

The The vessel walls are tracked through each frame by passing each frame and the row and column values from the ellipses found from the previous frame to the tracking function..

The tracking function uses "local snaking" i.e. the algorithm is more concerned with a snaxel's energy in relation to its adjacent snaxels rather than the energy of the snake as a whole based on the active couture model developed by Kass et al [11].

This was achieved by weighing the pixels in the search space according to optimal continuity and smoothness each respective pixel would provide(a higher weight indicates a better position) in addition to external energy.

The following equations were used to find the smoothness and continuity for each pixel respectively [12]:

$$E_{Smooth} = | P(x_{(i-1)}, y_{(i-1)}) - 2P(x_i, y_i) + P(x_{(i+1)}, y_{(i+1)}) | \quad (1)$$

$$E_{Cont} = || P_i - P_{(i+1)} | - | P_i - P_{(i-1)} | \quad (2)$$

where i is the index of the snaxel being analyzed and x and y are the x and y components of the appropriate snaxel .

The search space size was set to seventeen, this value was found semi-empirically (the size was chosen in such a way to not allow high snaxel velocity but the specific number was found by examining the output and determining what was the best value).

Next snaxel wandering due to the empty search space is eliminated by removing any snaxels that have either an empty search space or a search space that is out of bounds (exceeds image boundaries).

E. Determining Bifurcation Region

This paper focuses on finding the bifurcation region rather than a bifurcation point as there is no set convention for a bifurcation point (in image processing). This project defines the bifurcation region as the section of artery between the point where the internal and external arteries just touch and the point where the internal and external arteries effectively overlap to create the common carotid artery.

The program determines the bifurcation start by finding the centre of each ellipse by simply finding the midpoints between the smallest and largest row and column values for each ellipse respectively, finds the Euclidean length and the slope of the line that would join the two centers, and finds slope of this line relative to the slope of the major axis of each ellipse.

This slope is then used to find the distance from the centre of each ellipse to its respective border (at the points where the line that would connect the centre points bisects the borders) using the equation :

$$d = \sqrt{\frac{1}{\left(\frac{\sin\theta}{r_{major}}\right)^2 + \left(\frac{\cos\theta}{r_{minor}}\right)^2}} \quad (3)$$

If the sum of the two lengths found is greater than the length of the line that would join the two centers then the ellipses must be touching (no matter the orientation of the ellipses) and the bifurcation has therefore started.

The end of the bifurcation region is determined by finding the centre of each ellipse and finding the (absolute) difference between the two centers. If this difference is within acceptable margins (five pixels) the ellipses are considered to be overlapping and the bifurcation has therefore finished.

F. Determining Heart Rate

When the heart pumps blood through an artery, the artery distends (swells due to pressure from inside the vessel). This distension can be seen from the ultrasound images as a quick expansion (and subsequent contraction) in the artery wall which in turn will be reflected in the area of the ellipses detected.

For this reason, during the tracking sequence, the areas of the ellipses detected are calculated to create two 1D signals (one for each ellipse sequence) that can be processed to extract information relating to the heart rate.

These 1D signals contain information regarding the change in area due to the non uniformity of the artery and due to the distension and contraction. The former variations have a relatively low frequency and are filtered out by subtracting a low order best fit curve of the signal which produces a signal who's variations are only due to distension.

The function then counts a pulse after the first significant peak after a positive mean crossover. The heart rate is then calculated by multiplying the amount of pulses by the frame rate divided by the number of frames and multiplying by sixty (to get bpm).

G. Creating 3D Models

In order to create the 3D model the program simply stacks the row and column arrays of the tracked ellipses in the appropriate arrays. This effectively layers all the ellipses on top of each other. An array for the height component is also created which has equal spacing and a step for every frame processed.

III. RESULTS

A. The developed algorithms were tested using two different video sequences (Sample A and Sample B) of the carotid artery. These video sequences were captured using different machine models by different sonographers and had different orientations (on the XY plane) and time durations.3D Models

Figure 2 below shows the 3D model produced using Sample A. The transition from red to blue represents depth in the x direction.

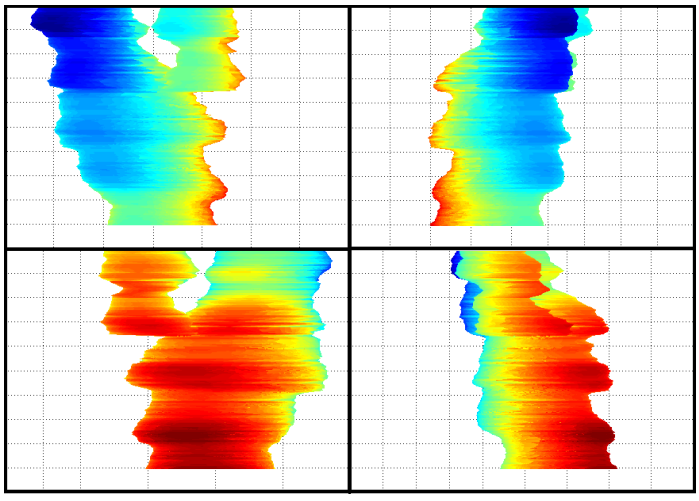

Figure 3: 3D Model of carotid artery

It can be seen from the figure above that there is what looks like ripple in the model, this is due to the distension that occurs when blood flows through the artery.

It can also be seen from the figure above that (excluding the ripple caused by distension and probe motion) the model is relatively accurate. However, inaccuracies still exist due to the fact that arteries are not perfectly elliptical.

B. Tracking

The program tracks through hundreds of frames so only selected frames that demonstrate its accuracy will be shown here. Figure 3 below demonstrates the snaxels (green pixels) conforming to the vessels' walls and the ellipses found (red pixels) based on the snaxels (sample A):

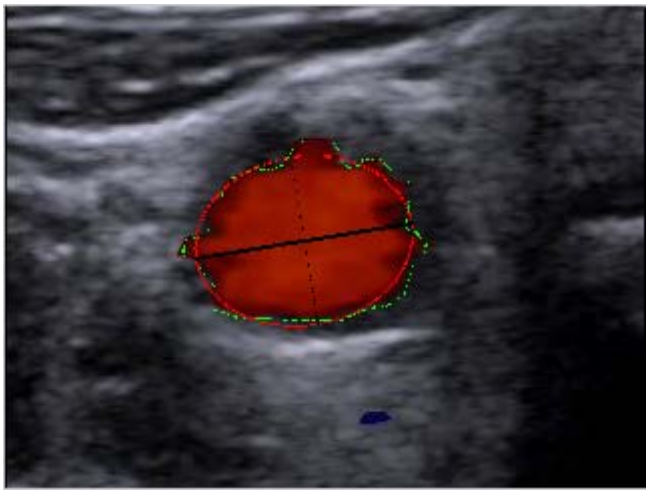

Figure 4: Tracking excerpt showing snaxel conformity

It can be seen from the figure above that, although the ellipses do not completely conform to the vessel, the snaxels hug the walls of the vessels accurately with an extremely low percentage of misplaced snaxels.

C. Bifurcation Detection

Figure 4 below shows the frame where the program detects the beginning of the bifurcation (sample A):

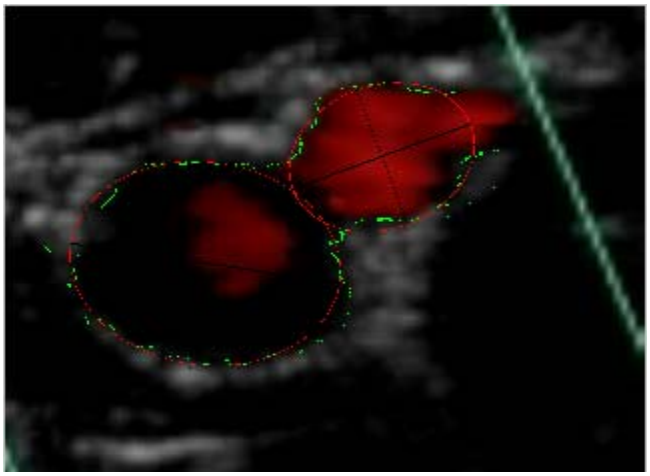

Figure 5: Frame detecting start of bifurcation

It can be seen from the figure above that the detection of the bifurcation does occur slightly after actual bifurcation. This is due to the criterion used for determination is that the ellipses must be partially overlapping.

The figure below shows the frame where the program detects the end of the bifurcation (sample A):

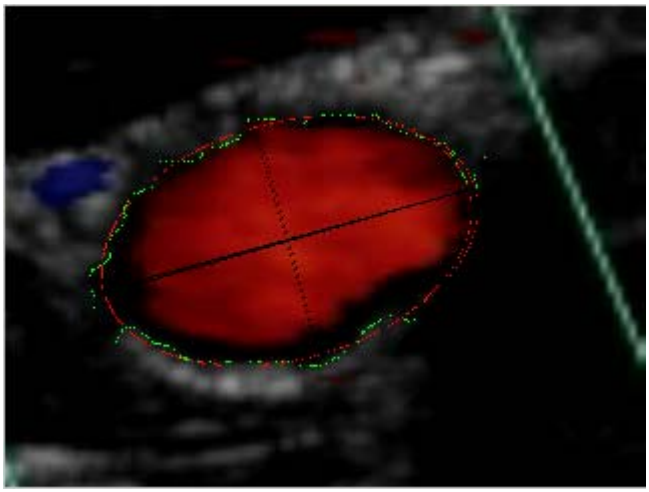

Figure 6: Frame where the end of bifurcation is detected

As can be seen from the figure above end of the bifurcation is determined when the two ellipses overlap.

The figure below shows a 3D model of the bifurcation region of the artery from different angles.

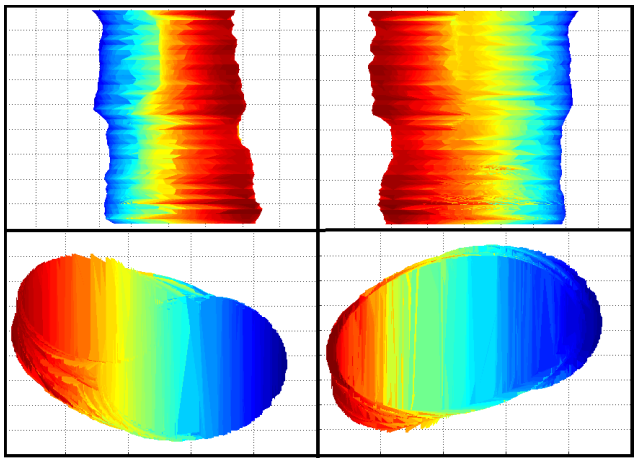

Figure 7: 3D model of bifurcation region from various angles

The transition from the converging external and internal carotid arteries to the common carotid artery can be seen from the top two tiles. The converging external and internal carotid arteries can be seen from the top view (third tile) and the common carotid artery can be seen from the bottom view (fourth tile).

D. Heart Rate Determination

The figure below is a plot of the magnitude of the area of each of the ellipses in sample B against the frame number:

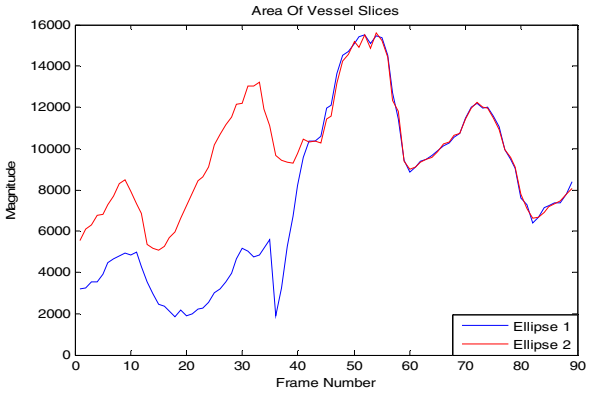

Figure 8: Area of vessel slices with respect to frame number

It can be seen from the figure above that the trend of each signal is the same (although the magnitudes can vary). Also it is evident that there is an offset in the magnitudes of the two signals at the start of the signal. The reason for this offset is that this is the region before the external and internal carotid arteries have converged into the common carotid artery and the external and internal carotid arteries are not the same size.

The two vessels converge to become the common carotid artery at frame forty (approximately). This is the cause for the magnitude offset decreasing dramatically (compared to the initial offset).

The low frequency component (the gentle rise and fall of the curve over the duration of the signal) is due to the vessel(s) getting larger and smaller. The high frequency component is due to the distension and subsequent contraction of the vessel(s) due to blood flow.

The figure below shows these signals after the heart rate detection algorithm removed the low frequency component and the point where the program has determined that a pulse is occurring.

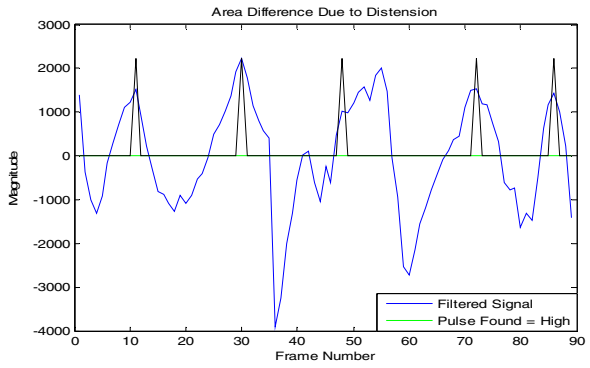

Figure 9: Variation in area due to distension & pulse detection

It can be seen from the plot above that the low frequency component has been, for the most part, removed from the signal.

It can also be seen from the figure above that five pulses were found for both signals and the resultant heart rate was found to be approximately eighty five beats per minute (for both signals - one shown here). The actual number of pulses that occur in the video was manually checked and found to be five proving the results to be accurate.

It can also be seen that the pulse spikes are not always in the optimum position (at the peak of distension) this does not pose a problem as the exact pulse position is not needed for the purposes of calculating heart rate (as the program only needs to determine the number of pulses as it has a priori knowledge of the time and frame rate).

IV. Conclusion

This paper demonstrates the efficacy of using local snakes to track transverse 2D ultrasound images in order to create 3D representations of the carotid artery (with the possibility of translation to other vessels), to determine bifurcation regions, and to ascertain heart rate. The outcome of the research surrounding this paper could be used as a basis for further study in the field of 3D reconstruction from 2D Ultrasound images and in the development of automated point of care testing in the domain of ultrasound sonography.

There are a multitude of different applications this work can be applied to including; automated determination of operation location for aneurysm surgery along a long vessel, aneurysm measurement, and determination of the distension coefficient which could aid in the detection of atherosclerosis among many more.

References

[1] "2011-12 Summary" NHS Abdominal Aortic Aneurysm Screening Programme.

[2] R. Erbel and H. Eggebrecht, "Aortic dimensions and the risk of dissection" *Heart (British Cardiac Society)*, vol. 92, no. 1, pp. 137–142, Jan. 2006.

[3] M. J. Bown, M. J. Sweeting, L. C. Brown, J. T. Powell, and S. G. Thompson, "Surveillance Intervals for Small Abdominal Aortic Aneurysms" *The Journal of the American Medical Association*, vol. 309, no. No. 8, pp. 806–813, Feb. 2013.

[4] M. Kuhn, R. L. Bonnin, M. J. Davey, J. L. Rowland, and S. L. Langlois, "Emergency department ultrasound scanning for abdominal aortic aneurysm: accessible, accurate, and advantageous" *Annals of emergency medicine*, vol. 36, no. 3, pp. 219–223, Sep. 2000.

[5] "Medicine Block 4:Skull and Neck," in *Baylor College of Medicine* .

[6] C. Finucane, J. Courtney, G. Boyle, and R. Kenny, "Toward A Technique for Ultrasound Guided Carotid Suinus Massage: An Image Processing Algorithm for Automated Bifurcation Detection" *(Unpublished)*.

[7] X. Yang, J. Jin, M. Xu, H. Wu, W. He, M. Yuchi, and M. Ding, "Ultrasound Common Carotid Artery Segmentation Based on Active Shape Model" *Comput. Math. Methods Med.*, vol. 2013, Mar. 2013.

[8] T. F. Cootes, C. J. Taylor, D. H. Cooper, and J. Graham, "Active shape models-their training and application"

Computational and Mathematical Methods in Medicine, vol. 61, pp. 38–59, 1995.

[9] D. C. Barratt, B. B. Ariff, K. N. Humphries, S. A. M. Thom, and A. D. Hughes, "Reconstruction and Quantification of the Carotid Artery Bifurcation From 3-D Ultrasound Images" *IEEE Transactions on Medical Imaging*, vol. 23, no. 5, pp. 567–83, 2004.

[10] J. Courtney and A. dePaor, "Direct Least-Squares Ellipse Fitting" *7th IASTED International Conference on Computer Graphics and Imaging*, Aug. 2004.

[11] M. Kass, A. Witkin, and D. Terzopoulos, "Snakes: Active Contour Models" *International Journal of Computer Vision*, vol. 1, no. 4, pp. 321–331, 1988.

[12] H. Tao, "Image Analysis and Computer Vision: Deformable Contours" Department of Computer Engineering, University of California at Santa Cruz.